



## ARTICLE



# Morphological and functional involvement of the inner retina in retinitis pigmentosa

Alessandro Arrigo<sup>1</sup> , Emanuela Aragona<sup>1</sup>, Cristian Perra<sup>2</sup>, Andrea Saladino<sup>1</sup>, Alessia Amato<sup>1</sup>, Lorenzo Bianco<sup>1</sup> , Adelaide Pina<sup>1</sup>, Giulia Basile<sup>1</sup>, Francesco Bandello<sup>1</sup> and Maurizio Battaglia Parodi<sup>1</sup>

© The Author(s), under exclusive licence to The Royal College of Ophthalmologists 2022

**BACKGROUND:** To investigate the morphological retinal parameters associated with retinal sensitivity status in retinitis pigmentosa (RP) through a quantitative multimodal imaging approach.

**METHODS:** The study was designed as an observational, prospective case series, including RP patients and healthy controls. Multimodal imaging included fundus autofluorescence (FAF), structural optical coherence tomography (OCT), OCT angiography (OCTA) and microperimetry (MP). The follow-up lasted 12 months. For each imaging modality, we performed an overall quantitative analysis and a detailed investigation based on the ETDRS-9 sectors grid. Quantitative parameters included the thickness of each retinal and choroidal layer, vessel density (VD), choriocapillaris porosity (CCP), FAF intensity and MP retinal sensitivity.

**RESULTS:** We included 40 eyes (40 patients) affected by RP and 40 healthy eyes (40 controls). Mean baseline BCVA was  $0.14 \pm 0.18$  LogMAR, with  $0.18 \pm 0.24$  LogMAR after 1-year of follow-up. RP eyes showed statistically significant alterations of retinal and choroidal layers on the ETDRS-9 sectors grid, significant reduction of VD values and MP retinal sensitivity, and significantly higher CCP than controls. The inner retinal layers proved closely associated with the functional integrity of the posterior pole. In addition, our ROC analysis provided quantitative cutoffs connected significantly with a high probability of observing a partial sparing of MP retinal sensitivity.

**CONCLUSIONS:** The inner retinal layers are closely associated with the functional integrity of the posterior pole in RP. FAF intensity reduction may be interpreted as lipofuscin metabolism impairment inducing increased phototoxic distress for retinal structures. Vascular involvement contributes to the morpho-functional deterioration of the macular region in RP.

*Eye* (2023) 37:1424–1431; <https://doi.org/10.1038/s41433-022-02139-7>

## INTRODUCTION


The term retinitis pigmentosa (RP) covers a heterogeneous group of inherited retinal disorders leading sufferers to experience progressive centripetal degeneration of the photoreceptors, followed by impaired dark adaptation, night blindness, progressive visual field loss, and variable involvement of the posterior pole [1]. Although RP is characterized by extensive genetically induced rod damage, cone photoreceptors are also well known to be considerably involved, mainly as a result of increased inflammation and oxidative stress [2]. This kind of degeneration leads to the progressive deterioration of central retinal sensitivity, as revealed by microperimetry (MP) [3, 4], with additional negative impact on patients' visual function and quality of life. The complexity of RP pathogenesis is further increased by evidence of intraretinal vascular network and choroidal network impairments, as detected by optical coherence tomography (OCT) and OCT angiography (OCTA) [5–7]. Previous structural OCT investigations have shown good correlations between the status of the outer retinal structures and the visual function of RP patients [8]. However, relatively recent studies also described a significant involvement of the inner retinal structures, which affect visual function and retinal sensitivity [9–12]. The causes of the inner

retinal changes are known in part: the main pathogen hypotheses focus on the effect of retinal remodelling induced by photoreceptor loss or the consequence of increased oxidative stress extending even to inner retinal structures. In addition, the posterior pole of RP eyes displays evident changes in the fundus autofluorescence (FAF) signal, which may be interpreted as the progressive loss of retinal pigments, with consequent increases in phototoxic damage to the retinal structures [13, 14].

In the present study, we performed a multimodal integrated quantitative investigation, including MP retinal sensitivity, structural OCT, OCTA and FAF, in order to assess the quantitative parameters strictly associated with decreased visual function and retinal sensitivity and to bring to light progression patterns over one year of follow-up.

## MATERIALS AND METHODS

The study was designed as an observational, prospective, case series with one year of follow-up. Consecutive patients with a genetically confirmed diagnosis of RP were recruited in the Retinal Heredodystrophy Unit of the Department of Ophthalmology of IRCCS San Raffaele Scientific Institute in Milan. The study was approved by the local ethical committee (NET-2016-

<sup>1</sup>Department of Ophthalmology, IRCCS San Raffaele Scientific Institute, Milan, Italy. <sup>2</sup>Department of Electrical and Electronic Engineering (DIEE), CNIT Research Unit, University of Cagliari, Cagliari, Italy. email: [alessandro.arrigo@hotmail.com](mailto:alessandro.arrigo@hotmail.com)

Received: 16 January 2022 Revised: 9 May 2022 Accepted: 10 June 2022

Published online: 29 June 2022

02363765), in accordance with the Declaration of Helsinki. Signed informed consent was obtained from each patient before being included the study.

The inclusion criteria were genetically confirmed diagnosis of RP and age > 18 years. The exclusion criteria were refractive errors greater than  $\pm 3D$ , high media opacity, macular atrophy, or other causes of poor fixation, present or past history of macular oedema, any other retinal and/or optic nerve diseases (e.g., diabetic retinopathy, glaucoma), any ophthalmic surgery in the 6 months prior to inclusion in the study, and any systemic conditions potentially affecting the analyses.

The ophthalmologic examination included best-corrected visual acuity (BCVA) measurement, using the standard Early Treatment Diabetic Retinopathy Study (ETDRS) chart, anterior and posterior segment slit-lamp evaluation, and Goldmann applanation tonometry. The quantitative assessment of FAF intensity, and structural OCT, OCTA and MP images included an overall analysis and a detailed investigation performed through an ETDRS-9 sectors grid (central, inner nasal, inner superior, inner temporal, inner inferior, outer nasal, outer superior, outer temporal, and outer inferior).

### Structural OCT analysis

Structural OCT images were acquired by means of a spectral-domain OCT instrument (Spectralis HRA2 + OCT, Heidelberg Engineering; Heidelberg, Germany). We included only high-quality images (ART > 25) and used the segmentation tool included in Heidelberg HEYEX device to measure the thickness of all retinal layers automatically on an ETDRS-9 sectors grid (central, inner nasal, inner superior, inner temporal, inner inferior, outer nasal, outer superior, outer temporal, and outer inferior). The tool was used under the supervision of two expert ophthalmologists (AA, EA), producing an ETDRS thickness map for the following layers: central macular thickness (CMT), retinal thickness (RT), retinal nerve fibre layer (RNFL), ganglion cell layer (GCL), inner plexiform layer (IPL), inner nuclear layer (INL), outer plexiform layer (OPL), outer nuclear layer (ONL), and ellipsoid zone thickness (EZ). In addition, the same graders performed the measures of choroidal thickness (CT), Haller layer thickness (HLT) and Sattler layer thickness (SLT). CT and HLT were obtained from a horizontal structural OCT scan centred on the fovea, calculating the mean value of five samples (subfoveal, 750  $\mu\text{m}$  and 1500  $\mu\text{m}$  nasal and temporal). SLT value corresponded to the result of (CT-HLT).

### OCTA analysis

OCTA acquisitions included 4.5  $\times$  4.5 mm and 12  $\times$  12 mm foveal scans, with Topcon quality index > 70 (Swept source DRI Triton Topcon, Topcon inc., Japan). We obtained the automatic segmentations of superficial capillary plexus (SCP), deep capillary plexus (DCP) and choriocapillaris (CC); all the reconstructions were carefully checked by two experts and manually modified if necessary (AA, EA). All the images were loaded in the ImageJ software package and in-house scripts were used to calculate vessel density (VD) [15], understood as the ratio between white and black pixels of the binarized OCTA images, with the subtraction of the foveal avascular zone area. We adopted a mean threshold to binarize all the images [16], choosing to calculate VD on 4.5  $\times$  4.5 mm scans so as to achieve the best compromise between the field of view and the resolution of the images. We also calculated the CC porosity (CCP) parameter as a measure of the flow voids in the CC, taking as our starting point binarized OCTA CC reconstructions and employing the porosity pipeline included in ImageJ to measure the CCP percentage [17].

### FAF and MP analyses

Blue-light FAF images were obtained by the same Spectralis HRA2 + OCT device (Heidelberg Engineering; Heidelberg, Germany). We developed an in-house tool to perform FAF intensity quantification based on the same ETDRS-9 sectors grid. A preliminary step was the normalization of all FAF images to obtain similar grayscale distribution. We then centred the ETDRS-9 sectors grid on the fovea and the algorithm provided the global FAF intensity within the grid and the values for each sector.

MP (MAIA, CenterVue, Padova, Italy) was carried out employing the 4–2 threshold strategy, with a 68-stimuli grid covering the central 10° of the retina, manually centred on the fovea by two experts (AP, LB) [18, 19]. In this case, we once again adopted an in-house tool to perform an ETDRS-9 sectors grid-based analysis of retinal sensitivity, including global and sector values.

All the measures were taken at baseline and after one year of follow-up, whereas MP retinal sensitivity was tested only at baseline. Although we

performed the detailed assessment of retinal layer thickness in all the sectors of the grid, to make the analyses easier to read and interpret we considered the mean values of the inner and outer sectors and treated mean inner values and mean outer values separately.

### Statistical analysis

The statistical analyses were performed using the SPSS software package (SPSS, Illinois, USA). Age and gender were considered fixed factors. In our univariate models, we used frequency histograms and quantile-quantile plots to test the normality distribution of each variable. Continuous variables were reported as mean  $\pm$  standard deviation, whereas frequency and proportions were described as categorical variables. We included only one randomly selected eye for each patient.

Continuous variables were analyzed by means of a two-tailed *T* test, and we used Pearson correlation analysis to assess the relationship between all the variables considered. The Bonferroni approach was employed to make multiple comparisons. As regards FAF intensity, while we considered the merged inner and outer FAF intensity values for the overall correlation analysis, we employed only the FAF values calculated in the inner ETDRS-9 grid sectors to examine the detailed correlation. We took this approach for three main reasons: (I) to avoid the possible influence of the hyperautofluorescent macular ring; (II) to avoid the possible effect of the central hypofluorescence typical of blue-light FAF; (III) to provide a reliable comparison with MP analysis, since the 68-stimuli MP grid is smaller than the ETDRS-9 grid, thus rendering the analysis of the outer sectors unreliable. Moreover, looking at the detailed correlation between MP values and retinal layer thicknesses, we considered only the correlations with central and inner ETDRS rings, so as to avoid possible pitfalls secondary to the inclusion of peripheral, potentially highly damaged posterior pole regions.

Since we included sixteen different variables, the statistical significance threshold was set at an alpha value  $< (0.05/16 = 0.003)$ . We also performed an ROC analysis to assess the presence of quantitative OCTA-based cutoffs associated with preserved retinal sensitivity. We built the model arbitrarily, assuming preserved retinal sensitivity to show MP values  $>$  (Mean of healthy controls/2 = 14 dB). The intraclass correlation coefficient (ICC) was calculated to assess the agreement between the two graders (overall 0.89; range 0.87–0.94).

## RESULTS

### Overall clinical characteristics

We included 40 eyes of 40 patients affected by RP (17 males; mean age 42  $\pm$  11 years) and 40 eyes of 40 healthy controls (20 males; mean age 42  $\pm$  8 years). The spectrum of RP-related genetic mutations is shown in Table 1. Mean baseline BCVA was 0.14  $\pm$  0.18 LogMAR, increasing to 0.18  $\pm$  0.24 LogMAR after 1-year of follow-up ( $p > 0.05$ ). All the clinical and imaging data are reported in Table 2. RP eyes displayed significantly worse BCVA and MP retinal sensitivity values, compared with healthy controls ( $p < 0.05$ ). CMT, CT and HLT were similar in all groups ( $p > 0.05$ ), whereas FAF intensity and SLT were significantly lower than in controls ( $p < 0.05$ ). Moreover, overall FAF intensity and MP retinal sensitivity was found to be significantly lower in RP than in healthy eyes ( $p < 0.05$ ). OCTA data for SCP, DCP and CC ( $p < 0.05$ ) showed that VD was significantly lower in RP than in control eyes. In addition, CCP was significantly higher in RP than in healthy eyes ( $p < 0.05$ ), while CVI was significantly lower in RP eyes than in controls ( $p < 0.05$ ). Baseline values turned out to be similar to those registered after 1-year ( $p > 0.05$ ), the only exception being SLT, which had undergone significant thinning after one year of follow-up ( $p < 0.05$ ).

### ETDRS-based quantitative analysis

The complete ETDRS analysis is shown in Supplementary Table 1, while the merged thickness analysis of inner and outer grids is shown in Table 3. Looking at the global values, RNFL, GCL, IPL, ONL and EZ were found to be significantly thinner in RP than in controls ( $p < 0.05$ ), whereas INL and OPL were significantly thicker in RP eyes ( $p < 0.05$ ). At the same time, FAF intensity and MP retinal sensitivity were significantly lower in RP than in control

**Table 1.** Genetic analysis in retinitis pigmentosa.

Gene	No. of patients
ABCA4	6
USH2A	10
PROM1	4
CYP4V2	2
NR2E3	2
PDE6A	1
RP1L1	2
RPGR	2
CNGA1	1
CNGB1	1
FSCN2	2
BBS1	1
RLBP1	2
MYO7A	1
CEPB90	1
EYE	1
EYS	1

eyes ( $p < 0.05$ ). A separate analysis of the inner rings confirmed these findings (all  $p < 0.05$ ), the only exception being RNFL, which largely matched healthy values ( $p > 0.05$ ). In contrast, looking at the outer ring values, we find that all the global findings were confirmed (all  $p < 0.05$ ) except for INL values, which proved analogous to those of healthy controls ( $p > 0.05$ ). We detected no significant changes in all the parameters after one year of follow-up (all  $p > 0.05$ ). The distribution of retinal layer thickness changes occurring in RP is plotted in Fig. 1. The detailed description for each layer is provided in the figure legend. Overall, all ETDRS sectors displayed considerable changes in retinal thickness and MP retinal sensitivity values; it is worth noting the evident alterations detected in sector S1 with regard to IPL thinning, INL and OPL thickening, and MP values (Fig. 1). RP eyes exhibited diffuse reductions in the FAF intensity pattern affecting both inner and outer sectors. Remarkably, an evident FAF intensity reduction was detected in the central sector (Fig. 1 and Supplementary Table 1).

### Correlation analysis

We have chosen to record the results of the correlation analysis separately.

If we look at each retinal layer's contribution to the full retinal thickness (Supplementary Table 2), we find our correlation analysis reveals that the nasal sectors behave differently to all the others in the ETDRS grid. Indeed, while both inner and outer retinal layers showed a correlation with the full retinal thicknesses in the superior, temporal and inferior sectors, the nasal sectors on the other hand displayed significant correlations only with inner retinal layers, especially as regards RNFL, GCL and IPL. This phenomenon was also confirmed by the correlation analysis assessing the relationship between MP retinal sensitivity values and all the retinal layers (Supplementary Table 3). Indeed, in this case too, nasal sectors showed significant MP retinal sensitivity relationships only with RNFL, GCL and IPL.

The correlation analysis considering the merged ETDRS grid values for all the parameters is shown in its entirety in Supplementary Table 4. As expected, MP retinal sensitivity showed a statistically significant correlation with LogMAR BCVA ( $p < 0.05$ ). Interestingly, looking at global MP retinal sensitivity values, as well as at the separated inner-outer rings values, MP significantly correlated both with inner and outer retinal layers. In particular,

**Table 2.** Mean clinical and imaging data.

	RP	Controls	<i>p</i> Value
No. of eyes	40	40	
Age	42 ± 11	42 ± 8	
Gender (M/F)	17/23	20/20	
LogMAR BCVA 0	0.14 ± 0.18	0.0 ± 0.0	<0.05*
LogMAR BCVA 1Y	0.18 ± 0.24		<0.05*
<i>p</i> Value	>0.05		
CMT 0	281 ± 50	278 ± 23	<i>p</i> > 0.05
CMT 1Y	279 ± 49		
<i>p</i> Value	>0.05		
FAF Intensity 0	113 ± 13	137 ± 5	<0.05*
FAF Intensity 1Y	110 ± 11		<0.05*
<i>p</i> Value	>0.05		
CT 0	243 ± 106	270 ± 67	>0.05
CT 1Y	238 ± 110		>0.05
<i>p</i> Value	>0.05		
SLT 0	55 ± 32	68 ± 23	<0.05*
SLT 1Y	48 ± 33		<0.05*
<i>p</i> Value	<0.05*		
HLT 0	189 ± 82	203 ± 60	>0.05
HLT 1Y	189 ± 85		>0.05
<i>p</i> Value	>0.05		
VD SCP 0	0.39 ± 0.03	0.41 ± 0.02	<0.05*
VD SCP 1Y	0.39 ± 0.03		<0.05*
<i>p</i> Value	>0.05		
VD DCP 0	0.34 ± 0.05	0.44 ± 0.01	<0.05*
VD DCP 1Y	0.34 ± 0.05		<0.05*
<i>p</i> Value	>0.05		
VD CC 0	0.49 ± 0.02	0.51 ± 0.01	<0.05*
VD CC 1Y	0.48 ± 0.02		<0.05*
<i>p</i> Value	>0.05		
CCP % 0	15 ± 5	4 ± 0.6	<0.05*
CCP % 1Y	15.5 ± 7		<0.05*
<i>p</i> Value	>0.05		
CVI 0	0.44 ± 0.28	0.65 ± 0.2	<0.05*
CVI 1Y	0.42 ± 0.26		<0.05*
<i>p</i> Value	>0.05		
Mean MP retinal sensitivity dB	11 ± 8	29 ± 3	<0.05*

Statistically significant values are marked by asterisks (\*). BCVA best-corrected visual acuity, CMT central macular thickness, CT choroidal thickness, FAF fundus autofluorescence, MP microperimetry, SLT Sattler layer thickness, HLT Haller layer thickness, VD vessel density, SCP superficial capillary plexus, DCP deep capillary plexus, CC choriocapillaris, CCP CC porosity, CVI choroidal vascularity index.

we found statistically significant correlations with RNFL, GCL, IPL, ONL and EZ, applying to both baseline and 1-year follow-up measurements (all  $p < 0.05$ ). It is noteworthy that the strongest correlations were found looking at inner retinal layers (RNFL, GCL and IPL), compared with outer retinal layers (ONL and EZ). FAF intensity values showed several statistically significant correlations with inner and outer retinal layers (all  $p < 0.05$ ). Conversely, based on our findings, FAF intensity has no significant relationship either with MP retinal sensitivity or LogMAR BCVA (both  $p > 0.05$ ). Lastly, LogMAR BCVA showed statistically significant correlations with

**Table 3.** ETRDRS grid merged sector analysis.

Inner + outer ETRDRS grid values		Inner ETRDRS grid values			Outer ETRDRS grid values						
Mean_All_RNFL_0	23 ± 8	27 ± 3	<0.05*	Mean_Inner_RNFL_0	22 ± 9	22 ± 3	>0.05	Mean_Outer_RNFL_0	27 ± 12	35 ± 5	<0.05*
Mean_All_RNFL_1Y	22 ± 9			Mean_Inner_RNFL_1Y	22 ± 9			Mean_Outer_RNFL_1Y	26 ± 14		
p Value	>0.05			p Value	>0.05			p Value	>0.05		
Mean_All_GCL_0	28 ± 12	40 ± 4	<0.05*	Mean_Inner_GCL_0	37 ± 18	52 ± 4	<0.05*	Mean_Outer_GCL_0	22 ± 10	37 ± 4	<0.05*
Mean_All_GCL_1Y	27 ± 12			Mean_Inner_GCL_1Y	36 ± 16			Mean_Outer_GCL_1Y	21 ± 10		
p Value	>0.05			p Value	>0.05			p Value	>0.05		
Mean_All_IPL_0	30 ± 7	35 ± 3	<0.05*	Mean_Inner_IPL_0	34 ± 11	42 ± 3	<0.05*	Mean_Outer_IPL_0	26 ± 5	31 ± 3	<0.05*
Mean_All_IPL_1Y	29 ± 7			Mean_Inner_IPL_1Y	34 ± 10			Mean_Outer_IPL_1Y	25 ± 6		
p Value	>0.05			p Value	>0.05			p Value	>0.05		
Mean_All_INL_0	38 ± 4	35 ± 3	<0.05*	Mean_Inner_INL_0	43 ± 6	41 ± 4	<0.05*	Mean_Outer_INL_0	32 ± 5	34 ± 3	>0.05
Mean_All_INL_1Y	37 ± 4			Mean_Inner_INL_1Y	42 ± 6			Mean_Outer_INL_1Y	31 ± 5		
p Value	>0.05			p Value	>0.05			p Value	>0.05		
Mean_All_OPL_0	34 ± 4	30 ± 3	<0.05*	Mean_Inner_OPL_0	38 ± 5	35 ± 5	>0.05	Mean_Outer_OPL_0	32 ± 5	27 ± 3	<0.05*
Mean_All_OPL_1Y	35 ± 5			Mean_Inner_OPL_1Y	38 ± 7			Mean_Outer_OPL_1Y	32 ± 5		
p Value	>0.05			p Value	>0.05			p Value	>0.05		
Mean_All_ONL_0	49 ± 11	72 ± 4	<0.05*	Mean_Inner_ONL_0	54 ± 14	74 ± 4	<0.05*	Mean_Outer_ONL_0	34 ± 8	63 ± 4	<0.05*
Mean_All_ONL_1Y	47 ± 10			Mean_Inner_ONL_1Y	53 ± 13			Mean_Outer_ONL_1Y	34 ± 9		
p Value	>0.05			p Value	>0.05			p Value	>0.05		
Mean_All_EZ_0	12 ± 8	22 ± 3	<0.05*	Mean_Inner_EZ_0	14 ± 6	22 ± 4	<0.05*	Mean_Outer_EZ_0	10 ± 12	16 ± 4	<0.05*
Mean_All_EZ_1Y	11 ± 10			Mean_Inner_EZ_1Y	13 ± 7			Mean_Outer_EZ_1Y	9 ± 11		
p Value	>0.05			p Value	>0.05			p Value	>0.05		
Mean_All_FAF_0	113 ± 13	132 ± 7	<0.05*	Mean_Inner_FAF_0	100 ± 23	131 ± 14	<0.05*	Mean_Outer_FAF_0	118 ± 14	141 ± 9	<0.05*
Mean_All_FAF_1Y	110 ± 11			Mean_Inner_FAF_1Y	97 ± 19			Mean_Outer_FAF_1Y	116 ± 13		
p Value	>0.05			p Value	>0.05			p Value	>0.05		
Mean_All_MP_0	11 ± 8	29 ± 3	<0.05*	Mean_Inner_MP_0	15 ± 8	28 ± 2	<0.05*	Mean_Outer_MP_0	9 ± 8	28 ± 2	<0.05*

These values are obtained from inner and outer sectors, excluding the central sector. Statistically significant values are marked by asterisks (\*). RNFL: retinal nerve fibre layer, GCL: ganglion cell layer, IPL: inner plexiform layer, INL: inner nuclear layer, ONL: outer plexiform layer, OPL: outer nuclear layer, EZ: ellipsoid zone thickness, FAF: fundus autofluorescence, MP: micropolymeretry.

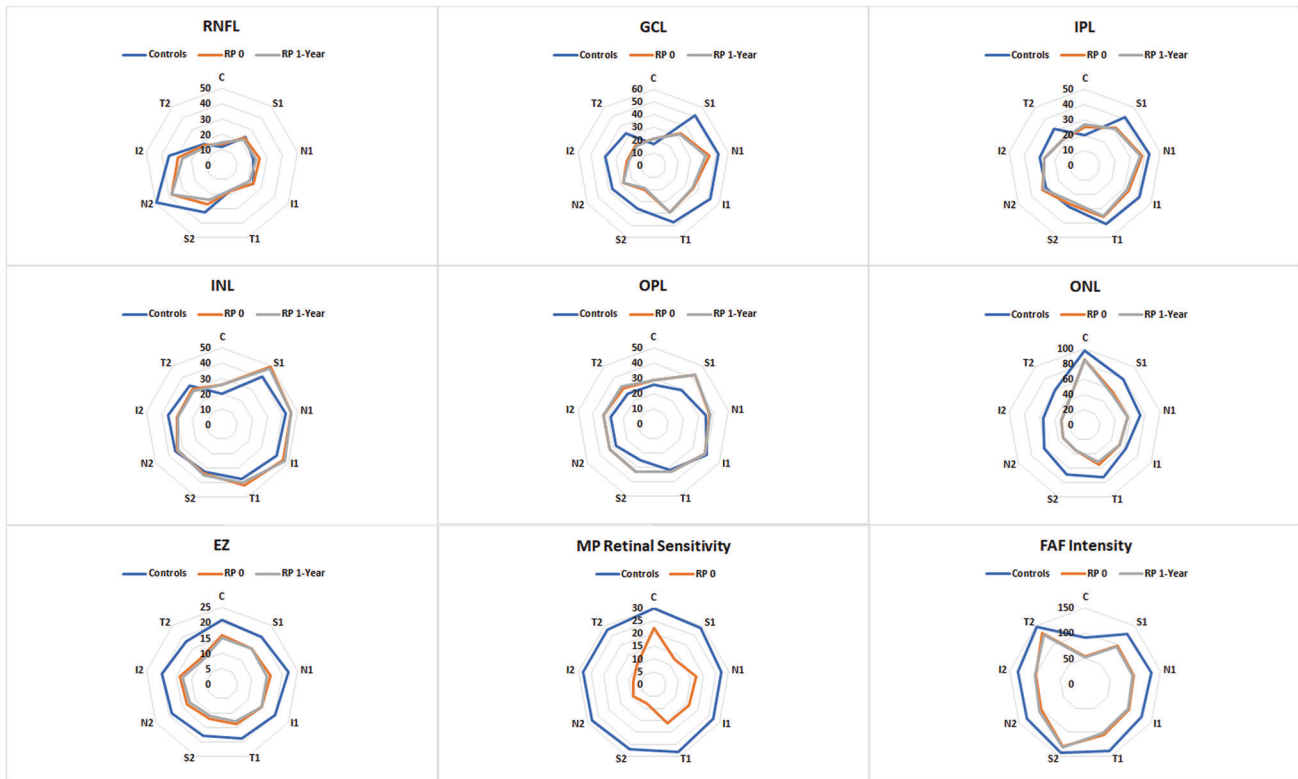


**Fig. 1 Radar plots of retinal layer thickness changes occurring in RP.** For each plot, healthy controls are shown in blue, RP values at baseline are shown in orange and RP values at 1-year follow-up are shown in grey. In RNFL the most extensive thinning occurs in S2, N2 and I2. Conversely, GCL is distinguished by diffuse thinning involving all the ETDRS grid sectors, the most pronounced being S1, S2, I1 and I2, with C being the only exception. IPL shows a diffuse thinning in S1, N1, I1, T1 and T2, whereas it is found to be thicker in C. Conversely, INL proves thicker overall in C, S1, N1, I1, T1, I2 and T2, whereas OPL turns out to be thicker in C, S1, S2, N2, I2 and T2. In both INL and OPL, the most pronounced changes are detected in S1. ONL and EZ prove to be thin throughout in RP. As regards MP retinal sensitivity, the lowest values are detected in the outer ring sectors. Interestingly, the most extensively affected inner sector is S1, while the others share similar MP values. Lastly, FAF displays reduced diffuse intensity, affecting both inner and outer sectors, and this reduction is curiously particularly marked in the C sector.

inner retinal layers (RNFL, GCL, IPL, INL and OPL) and with EZ (all  $p < 0.05$ ).

Looking at the contribution of vascular parameters to morphological and functional parameters (Supplementary Table 5), we found that SCP VD significantly correlated with LogMAR BCVA, DCP VD, CC VD, CCP and the thickness of the inner retinal layers. DCP VD significantly correlated with LogMAR BCVA, CC VD, CCP and the thickness of the following layers: GCL, IPL, INL, OPL, ONL and EZ. Remarkably, VD CC showed significant correlations with LogMAR BCVA, CCP, SLT, CVI and FAF intensity. Meanwhile, CCP showed a statistically significant relationship with LogMAR BCVA, SLT, CVI and with both inner and outer retinal thicknesses. In addition, MP retinal sensitivity significantly correlated with LogMAR BCVA, DCP VD, CC VD and CCP. No relevant genotype-phenotype correlations were found.

### ROC analysis

The ROC analysis was performed considering all the quantitative parameters collected. Meaningful findings were obtained with regard to RNFL, GCL, IPL, ONL, VD DCP, and CCP. In detail, our model revealed that MP retinal sensitivity values  $>14$  dB can be found on the basis of the following quantitative cutoffs: RNFL  $> 19.2 \mu\text{m}$  (sensitivity 0.95; specificity 0.79;  $p < 0.05$ ), GCL  $> 27.6 \mu\text{m}$  (sensitivity 0.98; specificity 0.82;  $p < 0.05$ ), IPL  $> 29.7 \mu\text{m}$  (sensitivity 0.98; specificity 0.80;  $p < 0.05$ ), ONL  $> 45.8 \mu\text{m}$  (sensitivity 0.89; specificity 0.71;  $p < 0.05$ ), VD DCP  $> 0.37$  (sensitivity 0.83; specificity 0.82;  $p < 0.05$ ) and CCP  $< 15.2\%$  (sensitivity 0.85; specificity 0.89;  $p < 0.05$ ).

We further inspected the correlation analysis on the basis of the results of the ROC analysis, considering only the correlations with a Pearson coefficient  $>0.7$ , and we record the most significant relationships in Table 4. Overall, MP retinal sensitivity is mainly associated with the integrity of RNFL and GCL; inner rings also showed a strong relationship with IPL and INL. The only significant vascular contribution came from the amount of CC flow voids.

### DISCUSSION

In the present study, we assessed the relationship between MP retinal sensitivity and quantitative structural OCT, OCTA and FAF alterations in a cohort of RP patients. In essence, RP was characterized by significantly thinner outer and inner retinal layers, reduced FAF intensity, increased intraretinal and choroidal vascular impairments, as well as reduced MP retinal sensitivity, compared with healthy controls. The most meaningful result was the relationship between MP retinal sensitivity and inner retinal layer thinning. In particular, RNFL, GCL, IPL and INL proved to be closely related to the functional integrity of the posterior pole. Remarkably, the morphological and vascular status of the outer retina were found to be less correlated with MP retinal sensitivity. Furthermore, FAF intensity showed no significant correlation with retinal sensitivity, whereas it was significantly associated with structural OCT and BCVA alterations.

With respect to OCTA findings, our data highlighted how retinal sensitivity is significantly associated with the integrity of the vascular network serving both inner and outer retinal layers,

**Table 4.** Filtered correlation analysis taking Pearson coeff. >0.7.

Mean MP Retinal Sensitivity dB Inner + Outer Rings	Parameter	Mean_RNFL_ALL_0	Mean_GCL_ALL_0	Mean_GCL_ALL_1Y	Porosity_CC_0	Porosity_CC_1Y
	Pearson coeff.	0.713	0.836	0.861	-0.867	-0.867
	p Value	<0.05*	<0.05*	<0.05*	<0.05*	<0.05*
Mean MP Retinal Sensitivity dB Inner Rings	Parameter	Mean_GCL_INNER_0	Mean_IPL_INNER_0	Mean_GCL_INNER_1Y	Mean_IPL_INNER_1Y	Mean_INL_INNER_1Y
	Pearson coeff.	0.837	0.767	0.858	0.752	0.728
	p Value	<0.05*	<0.05*	<0.05*	<0.05*	<0.05*
Mean MP Retinal Sensitivity dB Outer Rings	Parameter	Mean_RNFL_OUTER_0	Mean_GCL_OUTER_0	Mean_GCL_OUTER_1Y	Porosity_CC_0	Porosity_CC_1Y
	Pearson coeff.	0.752	0.844	0.852	-0.765	-0.890
	p Value	<0.05*	<0.05*	<0.05*	<0.05*	<0.05*

Statistically significant values are marked by asterisks (\*).

RNFL retinal nerve fibre layer, GCL ganglion cell layer, IPL inner plexiform layer, INL inner nuclear layer, CCP choriocapillaris porosity.

represented by VD values of DCP and CC. SCP showed significant relationships with inner retinal layer thickness but no correlations with retinal sensitivity. On the other hand, DCP and CC were strongly associated with the entire morpho-functional integrity of the retina in RP. In addition, these parameters provided clinically relevant cutoffs associated with the partial sparing of MP retinal sensitivity values. In particular, a retinal status displaying RNFL > 19.2  $\mu\text{m}$ , GCL > 27.6  $\mu\text{m}$ , IPL > 29.7  $\mu\text{m}$ , ONL > 45.8  $\mu\text{m}$ , VD DCP > 0.37 and CCP < 15.2% was associated with a high probability of having MP retinal sensitivity values >14 dB.

We found that the vascular and the non-vascular compartments are strictly interconnected and related with the degenerative mechanisms typical of RP and their progression. However, our analyses highlighted two novel and potentially clinically relevant features: (I) the integrity of the RPE-photoreceptor complex has a minor role in defining retinal sensitivity, as far as the inner retinal layers are concerned; (II) the functional complex made up of RNFL, GCL, IPL and INL plays a major role in RP; (III) although representing secondary phenomena, intraretinal and choroidal vascular status further reinforce morpho-functional retinal integrity in RP.

Many studies have already demonstrated the importance of GCL integrity in preserving the visual function [20, 21], and a study based on multifocal electroretinography (mfERG) has shown that mfERG signal preservation is strictly related to the integrity of GCL in RP [22]. From this point of view, the present investigation represents the first report suggesting a relationship between GCL impairment and retinal sensitivity loss in RP. About this point, GCL involvement in RP has been already demonstrated by histologic investigations, reporting a remarkable loss both of IPL and GCL [9]. This phenomenon is part of a much more complex cascade of events occurring in RP, causing an intense retinal remodelling involving retinal neurons and glial cells [9]. These cytotypes are responsible of many functions, including the processing of the visual information. For this reason, although we are aware that our in vivo findings cannot reach a sufficient level of evidence to demonstrate a clear relationship, we may advance the hypothesis that GCL impairment is associated with a loss of retinal sensitivity.

However, there is no consensus regarding thickening or thinning of inner retinal layers in RP [23]. In the present investigation, all retinal layers proved to be significantly thinner in RP than in healthy controls, excepting the INL and OPL, which turned out to be significantly thicker in RP. The increased thickness of the INL in RP has already been described [24] and interpreted as typical of retinal regions affected by photoreceptors loss [25]. However, in the present study, INL was found to be more closely associated with the functional integrity of the retina than the RPE-photoreceptor complex, thus suggesting INL thickening is an early biomarker of central involvement in RP. In addition, we also record a significant thickening of OPL, which might be interpreted as a sign of Henle fibre swelling secondary to an inadequate energy supply or cystic degeneration [26]. We have provided a picture of the sectorial ETDRS-based involvement of each retinal layer, showing that some layers, especially INL and OPL, showed asymmetric changes – more pronounced in S1 than in the other sectors. Similar behaviour was found in MP values, thus supporting the hypothesis that morpho-functional changes follow a sectorial progression RP. However, our data are not sufficient to reach more reliable conclusions, thus making this an interesting topic for future studies.

The FAF value was found to have decreased in RP at the posterior pole, compared with healthy controls. On this basis, we might speculate that the overall reduction of FAF intensity, as described in the present study, might be interpreted as a sign of metabolic dysregulation occurring at the posterior pole, with increased phototoxic distress affecting both RPE and photoreceptors [13, 27]. Conversely, the development of the

hyperautofluorescent ring occurs independently of the overall FAF intensity reduction, which we interpret largely as a reactive phenomenon related to the deteriorated visual function in RP [13, 27]. It is also worth noting that a considerable reduction in FAF intensity was detected in the central ETDRS sector. The foveal region is well known to contain melanin rather than lipofuscin pigment. Although near-infra-red autofluorescence assessment would have provided more specific results concerning central FAF, the significant decrease in central FAF intensity described in the present study reinforces previous findings that also detected a notable involvement of foveal pigment metabolism in RP [28]. Furthermore, MP was not influenced by FAF intensity. This would mean that pigment changes occur independently of the progression of the functional alterations. However, nothing definitive can be said at this juncture and we acknowledge that the topic would benefit from further dedicated investigations.

It was our aim in this study to explore a widely debated topic, namely the role of vascular impairment in RP. There is no doubt that intraretinal capillaries and choroidal vessels are impaired in RP, as several studies have pointed out [5–7]. Even so, the “chicken or egg” question is yet to be answered. RP is first and foremost an outer retinal, genetically determined disorder. The RPE-photoreceptor complex is fundamental not only for capturing and transducing the visual signal, but also for the regulation of the outer retinal vascular compartment, represented by the CC-choroidal interface [29]. The vascular endothelial growth factor (VEGF) released by the RPE plays a crucial role in supporting the integrity of the CC [30]. Moreover, endogenous VEGF is needed to promote the survival of glial cells and photoreceptors [31–33]. The RP-related dysregulation of the outer retinal homeostasis might be responsible for the CCP increases detected in the present study, which we interpret as a potential early sign of CC impairment. With respect to CC VD and choroidal alterations, mainly represented by SLT thinning and CVI reduction, these occur as RP progresses towards more advanced stages. The other side of the coin is represented by inner retinal vascular alterations. Intraretinal vessel perfusion is mainly controlled by blood pressure regulation and local factors, involving retinal neurons and glial cells [34–36], which in this context cover several fundamental roles in the regulation of the intraretinal vascular network [34–36]. For this reason, we can assume that the impairment of inner retinal cytotypes, causing the detected thinning or thickening of retinal layers, associated with the reduction of growth and regulatory factors, might represent a pathogenic source of SCP and DCP dropout. It thus seems possible to draw the conclusion that vascular involvement is a secondary pathogenic source of source of di RP, caused by the combined impairment of inner and outer retinal sources of VEGF and of overall drops in retinal metabolism.

In this very complex scenario, the decreased visual function typical of RP cannot be considered a mere consequence of photoreceptor loss, but the result of an intricate cascade of events leading to the loss of both inner and outer retinal homeostasis.

We are aware that our study is handicapped by a number of shortcomings, principally associated with the limited number of eyes and the short follow-up. We also realize that all imaging modalities may be affected by artifacts. We have tried to sidestep this eventuality by including only high-quality images and by introducing pre-processing steps to normalize images originating from different eyes. We are confident this has made our analyses more reliable. MP investigation was performed only at baseline and no other functional investigations, above of all electrophysiologic tests, were carried out. For all these reasons, further, histologically validated studies are warranted to draw more definite conclusions.

To sum up, our study reported the overall quantitative morpho-functional status characterizing a cohort of RP eyes. Although originating from genetically determined damage to

the RPE-photoreceptor complex, RP pathogenesis is distinguished by major involvement of RNFL, GCL, IPL and INL. These layers play a leading role in determining retinal sensitivity status and showed statistically significant quantitative cutoffs associated with a functionally partially spared retina. The vascular compartment is implicated in RP, although representing a secondary pathogenic source of RP-related damage and a cause of disease progression. Macular lipofuscin changes contribute to the central phototoxic distress but have no direct relationship with the functional status of the retina.

## SUMMARY

What was known before

- Retinitis pigmentosa is a peripheral outer retinal disorder.

What this study adds

- We found a significant morpho-functional involvement also of the posterior pole.
- Inner retinal showed significant alterations and it was more associated with retinal sensitivity values than outer retina.
- Our findings provide new insights about the extremely complex pathogenesis of retinitis pigmentosa, highlighting this should not be merely considered an outer retinal disorder.

## DATA AVAILABILITY

Data may be available after formal request to the corresponding author.

## REFERENCES

1. Hartong DT, Berson EL, Dryja TP. Retinitis pigmentosa. *Lancet*. 2006;368:1795–809.
2. Campochiaro PA, Mir TA. The mechanism of cone cell death in retinitis pigmentosa. *Prog Retina Eye Res*. 2018;62:24–37.
3. Iftikhar M, Kherani S, Kaur R, Lemus M, Nefalar A, Usmani B, et al. Progression of retinitis pigmentosa as measured on microperimetry: the PREP-1 study. *Ophthalmol Retina*. 2018;2:502–7.
4. Buckley TMW, Jolly JK, Josan AS, Wood LJ, Cehajic-Kapetanovic J, MacLaren RE. Clinical applications of microperimetry in RPGR-related retinitis pigmentosa: a review. *Acta Ophthalmol*. 2021;99:819–25.
5. Iacono P, Parodi MB, La Spina C, Zerbini G, Bandello F. Dynamic and static vessel analysis in patients with retinitis pigmentosa: a pilot study of vascular diameters and functionality. *Retina*. 2017;37:998–1002.
6. Arrigo A, Romano F, Albertini G, Aragona E, Bandello F, Battaglia Parodi M. Vascular patterns in retinitis pigmentosa on swept-source optical coherence tomography angiography. *J Clin Med*. 2019;8:1425.
7. Arrigo A, Bordato A, Romano F, Aragona E, Grazioli A, Bandello F, et al. Choroidal patterns in retinitis pigmentosa: correlation with visual acuity and disease progression. *Transl Vis Sci Technol*. 2020;9:17.
8. Battaglia Parodi M, La Spina C, Triolo G, Riccieri F, Pierro L, Gagliardi M, et al. Correlation of SD-OCT findings and visual function in patients with retinitis pigmentosa. *Graefes Arch Clin Exp Ophthalmol*. 2016;254:1275–9.
9. Jones BW, Pfeiffer RL, Ferrell WD, Watt CB, Marmor M, Marc RE. Retinal remodeling in human retinitis pigmentosa. *Exp Eye Res*. 2016;150:149–65.
10. Funatsu J, Murakami Y, Nakatake S, Akiyama M, Fujiwara K, Shimokawa S, et al. Direct comparison of retinal structure and function in retinitis pigmentosa by co-registering microperimetry and optical coherence tomography. *PLoS ONE*. 2019;14:e0226097.
11. Jasleen KJ, Moreno M, Piers AJ, Thomas MWB, Holly B, MacLaren RE, et al. Inner retinal thickening affects microperimetry thresholds in the presence of photoreceptor thinning in patients with RPGR retinitis pigmentosa. *Br J Ophthalmol*. 2020;bjophthalmol-2020-317692.
12. Hara A, Nakazawa M, Saito M, Suzuki Y, Lewin AS. The qualitative assessment of optical coherence tomography and the central retinal sensitivity in patients with retinitis pigmentosa. *PLoS ONE*. 2020;15:e0232700.

13. Schuerch K, Woods RL, Lee W, Duncker T, Delori FC, Allikmets R, et al. Quantifying fundus autofluorescence in patients with retinitis pigmentosa. *Investig Ophthalmol Vis Sci.* 2017;58:1843–55.
14. Dysli C, Schuerch K, Escher P, Wolf S, Zinkernagel MS. Fundus autofluorescence lifetime patterns in retinitis pigmentosa. *Invest Ophthalmol Vis Sci.* 2018;59:1769–78.
15. Schindelin J, Arganda-Carreras I, Frise E, Kaynig V, Longair M, Pietzsch T, et al. An open-source platform for biological-image analysis. *Nat Methods.* 2012;9:676–82.
16. Arrigo A, Aragona E, Saladino A, Amato A, Bandello F, Battaglia Parodi M. The impact of different thresholds on optical coherence tomography angiography images binarization and quantitative metrics. *Sci Rep.* 2021;11:14758.
17. Parodi B, Nieto A, Albrecht V, Maas J, Orth M, Neumaier K, et al. Multimodal imaging in subclinical best vitelliform macular dystrophy. *Br J Ophthalmol.* 2020;15:19. [bjophthalmol-2020-317635](https://doi.org/10.1136/bjophthalmol-2020-317635).
18. Parodi MB, Triolo G, Morales M, Borrelli E, Cicinelli MV, Cascavilla ML, et al. MP1 and MAIA fundus perimetry in healthy subjects and patients affected by retinal dystrophies. *Retina.* 2015;35:1662–9.
19. Battaglia Parodi M, Castellino N, Iacono P, Chowers I, Empeslidis T, Goldstein M, et al. Microperimetry in Best vitelliform macular dystrophy. *Retina.* 2018;38:841–8.
20. Kim JH, Lee HS, Kim NR, Seong GJ, Kim CY. Relationship between visual acuity and retinal structures measured by spectral domain optical coherence tomography in patients with open-angle glaucoma. *Investig Ophthalmol Vis Sci.* 2014;55:4801–11.
21. Rebolleda G, Sánchez-Sánchez C, González-López JJ, Contreras I, Muñoz-Negrete FJ. Papillomacular bundle and inner retinal thicknesses correlate with visual acuity in nonarteritic anterior ischemic optic neuropathy. *Invest Ophthalmol Vis Sci.* 2015;56:682–92.
22. Vamos R, Tatrai E, Nemeth J, Holder GE, DeBuc DC, Somfai GM. The structure and function of the macula in patients with advanced retinitis pigmentosa. *Investig Ophthalmol Vis Sci.* 2011;52:8425–32.
23. Liu G, Liu X, Li H, Du Q, Wang F. Optical coherence tomographic analysis of retina in retinitis pigmentosa patients. *Ophthalmic Res.* 2016;56:111–22.
24. Nagasaka Y, Ito Y, Ueno S, et al. Inner retinal layer thickness in eyes with retinitis pigmentosa. *Invest Ophthalmol Vis Sci.* 2014;55:1725.
25. Huang WC, Cideciyan AV, Roman AJ, Sumaroka A, Sheplock R, Schwartz SB, et al. Inner and outer retinal changes in retinal degenerations associated with ABCA4 mutations. *Investig Ophthalmol Vis Sci.* 2014;55:1810–22.
26. Bringmann A, Reichenbach A, Wiedemann P. Pathomechanisms of cystoid macular edema. *Ophthalmic Res.* 2004;36:241–9.
27. Lee J, Asano S, Inoue T, Fujino Y, Matsuura M, Kitamoto K, et al. Investigating the usefulness of fundus autofluorescence in retinitis pigmentosa. *Ophthalmol Retin.* 2018;2:1062–70.
28. Kellner U, Kellner S, Weber BH, Fiebig B, Weinitz S, Ruether K. Lipofuscin- and melanin-related fundus autofluorescence visualize different retinal pigment epithelial alterations in patients with retinitis pigmentosa. *Eye.* 2009;23:1349–59.
29. Kornfield TE, Newman EA. Regulation of blood flow in the retinal trilateral vascular network. *J Neurosci.* 2014;34:11504–13.
30. Saint-Geniez M, Kurihara T, Sekiyama E, Maldonado AE, D'Amore PA. An essential role for RPE-derived soluble VEGF in the maintenance of the choriocapillaris. *Proc Natl Acad Sci USA.* 2009;106:18751–6.
31. Saint-Geniez M, Maharaj ASR, Walshe TE, Tucker BA, Sekiyama E, Kurihara T, et al. Endogenous VEGF is required for visual function: evidence for a survival role on müller cells and photoreceptors. *PLoS ONE.* 2008;3:e3554.
32. Froger N, Matonti F, Roubeix C, Forster V, Ivkovic I, Brunel N, et al. VEGF is an autocrine/paracrine neuroprotective factor for injured retinal ganglion neurons. *Sci Rep.* 2020;10:12409.
33. Hu J, Zhu M, Li D, Wu Q, Le YZ. VEGF as a direct functional regulator of photoreceptors and contributing factor to diabetes-induced alteration of photoreceptor function. *Biomolecules.* 2021;11:988.
34. Tani T, Nagaoka T, Nakabayashi S, Yoshioka T, Yoshida A. Autoregulation of retinal blood flow in response to decreased ocular perfusion pressure in cats: comparison of the effects of increased intraocular pressure and systemic hypotension. *Investig Ophthalmol Vis Sci.* 2014;55:360–7.
35. Weerasekera LY, Balmer LA, Ram R, Morahan G. Characterization of retinal vascular and neural damage in a novel model of diabetic retinopathy. *Investig Ophthalmol Vis Sci.* 2015;56:3721–30.
36. Newman EA. Glial cell regulation of neuronal activity and blood flow in the retina by release of gliotransmitters. *Philos Trans R Soc Lond B Biol Sci.* 2015;370:20140195.

## AUTHOR CONTRIBUTIONS

AA, EA: study design, study conduction, data analysis, data interpretation, manuscript draft. CP, AS, AA, LB, AP, GB: data acquisition, data analysis, revision of the literature, critical revision of the manuscript. FB, MBP: data interpretation, critical revision of the manuscript, supervision of the entire study.

## FUNDING

FB consultant for: Alcon (Fort Worth, TX, USA), Alimera Sciences (Alpharetta, GA, USA), Allergan Inc (Irvine, CA, USA), Farmila-Thea (Clermont-Ferrand, France), Bayer Shering-Pharma (Berlin, Germany), Bausch And Lomb (Rochester, NY, USA), Genentech (San Francisco, CA, USA), Hoffmann-La-Roche (Basel, Switzerland), NovagaliPharma (Évry, France), Novartis (Basel, Switzerland), Sanofi-Aventis (Paris, France), Thrombogenics (Heverlee, Belgium), Zeiss (Dublin, USA). All other authors have no disclosures to declare.

## COMPETING INTERESTS

The authors declare no competing interests.

## ADDITIONAL INFORMATION

**Supplementary information** The online version contains supplementary material available at <https://doi.org/10.1038/s41433-022-02139-7>.

**Correspondence** and requests for materials should be addressed to Alessandro Arrigo.

**Reprints and permission information** is available at <http://www.nature.com/reprints>

**Publisher's note** Springer Nature remains neutral with regard to jurisdictional claims in published maps and institutional affiliations.